Hindawi Publishing Corporation
Journal of Nanomaterials
Volume 2013, Article ID 514917, 8 pages
http://dx.doi.org/10.1155/2013/514917

Research Article

Efficient Removal of Cr(VI) with Fe/Mn Mixed Metal Oxide Nanocomposites Synthesized by a Grinding Method

Wang Weilong[1] and Fu Xiaobo[2]

[1] *Center for Energy Conservation Technology, School of Engineering, Sun Yat-sen University, Guangzhou 510006, China*
[2] *Department of Chemistry, School of Life Science and Technology, Jinan University, Guangzhou 510632, China*

Correspondence should be addressed to Fu Xiaobo; txiaobofu@jnu.edu.cn

Received 5 January 2013; Accepted 13 February 2013

Academic Editor: Huijun Wu

Fe/Mn mixed metal oxides were synthesized facilely by a grinding method and were characterized by TEM, XRD, XPS, and BET. The characterization results revealed that mixed metal oxides were mainly composed of not highly crystallized Fe_2O_3 and Mn_3O_4 nanoparticles with a diameter about 3–5 nm. The specific BET surface areas of the composite were affected by the amounts of KCl diluent in the preparation process and about 268 m^2/g of the composite can be achieved. Compared with metal oxide adsorbents existent, the composites showed good adsorption capacity, stability, and regeneration activity for Cr(VI) removal. The enhanced adsorption capacity was speculated to be ascribed to the synergistic effect of the mixed metal oxides. By monitoring the valence change in the adsorption process using XPS characterization, the mechanism for Cr(VI) removal on the composites was found to be a combination of electrostatic attraction and ion exchange. The above results demonstrated that the synthesized metal oxides nanocomposite is of great potential for Cr(VI) removal in the fields of remediation of environmental problems.

1. Introduction

In the past years, the removal of heavy metals from industrial waste water streams has been widely studied due to the high threat of such pollutants to public health and environment [1–4]. The contamination of hexavalent chromium species is a major problem in many industrial areas, such as electroplating and metal finishing industries [5–7]. With the development of the stringent ecological standards, it is urgent for these industries to reduce the chromium in their effluents to an acceptable level before discharging into municipal sewers. Various methods have been developed to remove the chromium from industrial waste water, such as chemical redox followed by precipitation, ion exchange, and reverse osmosis. However, these methods have many drawbacks [8]. Currently, for large-scale used chemical redox method, a major drawback related to precipitation is slurry production. Both ion exchange and reverse osmosis methods are not economically attractive as a result of their high operating costs [8]. Recently, adsorption has been recognized as one of the most promising techniques for removal of chromium and its effectiveness has been demonstrated [5–7, 9].

In the whole adsorption process, the adsorbents play an important role. How to choose a suitable adsorbent is still a challenge. Several efforts have been devoted to the synthesis of a series of adsorbents. In general, a good adsorbent should not only process high adsorption efficiency but also be regenerated. Activated carbon, processing high BET surface areas, was adopted as an adsorbent to remove the heavy metals and better adsorption efficiency was achieved [10]. However, activated carbon which was commonly used by commercial regenerators was regenerated at a rather high temperature. Ho et al. [11] found that *Sphagnum* peat moss is an effective adsorbent for hexavalent chromium and 50% of chromium recovery was obtained. Srivastava [12] discovered that sawdust is effective for removal of hexavalent chromium and other heavy metals. These adsorbents also have a disadvantage which is that they could not be regenerated. Therefore, the search of new adsorbents for the removal of hexavalent chromium has directed attention

to synthesize new materials with high adsorption efficiency and good regeneration ability. Meanwhile, the development of nanoscience and nanotechnology is expected to provide a solution for the remediation of environmental problems. Thus, the design and application of novel nanomaterials for environmental protection have been receiving more and more attention in recent years.

Now, several researchers have focused on metal oxide nanoparticles and their composites for their high BET surface areas and fast adsorption kinetics when subjecting to the treatment of chromium from waste water. Zhong et al. [13, 14] use 3d flowerlike Fe_2O_3 nanostructures as adsorbents for the removal of Cr(VI). Compared with the commercial Fe_2O_3 particles, 3d flowerlike Fe_2O_3 nanostructures exhibit higher adsorption capacity. Chen et al. [15, 16] and his group found that magnetite and γ-Fe_2O_3 nanoparticles showed high adsorption capacity for Cr(VI) removal (about 19.4 mg/g). Meanwhile, the adsorption capacity of the γ-Fe_2O_3 particles can be enhanced by modifying the surface properties of the particles with MnO_2 [17]. After that, they coated the γ-Fe_2O_3 nanoparticles with a layer of FeOOH and the adsorption capacity for Cr(VI) was improved (about 25.6 mg/g) [18]. These results demonstrate that mixed metal oxide nanocomposites possess high adsorption capacity for removal of Cr(VI). The development of metal oxide nanocomposites, which can be used as adsorbent for Cr(VI), is of both economic and environmental significance. A growing number of methods, such as coprecipitation, sol-gel, hydrothermal methods, were involved to solve the problem. As some of mechanochemical syntheses show great potential with regards to not only energy saving and reducing cost but also improved safety, this technology should prove to be highly attractive when substituting methods of preparing conventional adsorbent [19].

In this paper, we use a grinding method to synthesize the Fe/Mn mixed oxides nanocomposites with high BET surface areas. The synthesized composites were applied in the removal of Cr(VI) and the high adsorption capacity, stability, and regeneration ability of the product were achieved. It is expected that the insight provided by this study will contribute to the Cr(VI) removal from the waste water.

2. Experimental

All chemical stock solutions were prepared from reagent-grade chemicals using Millipore ultrapure water. $NaNO_3$, NaOH, HNO_3, $Fe(NO_3)_3{\cdot}6H_2O$, $MnCl_2{\cdot}4H_2O$, KOH, KCl, and K_2CrO_4 were purchased from Sigma-Aldrich and used without further purification.

2.1. Materials Preparation. For the synthesis of mixed metal oxide nanocomposites, 6.986 g $Fe(NO_3)_3{\cdot}6H_2O$ and 1.979 g $MnCl_2{\cdot}4H_2O$ and KCl powders (with different ratio of $MnCl_2$ to KCl) were mixed together and ground to a very fine powder using an automatic electrical mortar at room temperature for 10 min. The mixture obtained from the grinding was a brown paste. To the mortar was added KOH powder, followed by grinding for another 30 min at room temperature. A significant amount of heat and some vapor was given off in the first few minutes of the KOH addition. After the reaction, the resultant composite was diluted by DI water, then filtered and washed with DI water repeatedly until no Cl^- could be detected. The precipitate was collected and dried in an oven at 70°C overnight. A comparison experiment was conducted by using $Fe(NO_3)_3{\cdot}6H_2O$ or $MnCl_2{\cdot}4H_2O$ as only the starting material.

2.2. Materials Characterization. The resultant composites were characterized by powder X-ray diffraction (XRD), BET, X-ray photoelectron spectroscopy (XPS), and high resolution transmission electron microscopy (HRTEM). XRD measurements were conducted on a PAnalytical X'Pert Pro X-ray Diffractometer equipped with Cu-Kα radiation (λ = 1.54178 Å), applying 40 kV voltage and 40 mA current. The BET specific surface area was determined by N_2 adsorption at 77 K using a Micromeritics ASAP 2000 system after the sample was degassed in vacuum at 130°C overnight. XPS spectrum was obtained in a Physical Electronics Corporation PHI 5600 machine with Al Kα radiation (350 W) under 10^{-7} Pa and calibrated internally by carbon deposit C_{1s} (285.0 eV). TEM observation was carried out on a JEOL JEM-2010F electron microscope equipped with a Bruker Energy Dispersive Spectrometer (EDS). The amount of iron and manganese leaching from the composites was measured using ICP-AES (Perkin Elmer Optima-3000XL). The concentration of the Cr(VI) was measured using an UV-Vis spectrometer (Shimadzu UV-Vis 5000) according to the diphenyl carbazide method [20].

2.3. Adsorption Capacity Test. The experimental procedures were according to the processes reported by Hu et al. [16–18]. The adsorption studies were performed by mixing 0.2 g nanocomposites with 40 mL K_2CrO_4 solution of varying concentration in a 100 mL stopper conical flask. The pH of the suspensions was adjusted using 0.1 M HNO_3 and 0.1 M NaOH solutions. All of the Cr(VI) solutions have a matrix of 0.1 M $NaNO_3$ to keep the ion strength relatively constant. All the adsorption experiments were carried out at 25°C, pH 2, and shaking rate of 200 rpm unless stated otherwise. Adsorption equilibrium studies were conducted by shaking 20 mL of Cr(VI) solution at initial concentrations varying from 10 to 200 mg/L and 0.1 g of adsorbent nanoparticles. To study the stability of the adsorbent, 0.01 M NaOH solution was used as eluant and five cycles of adsorption-desorption processes were carried out. For each cycle, 40 mL of 100 mg/L Cr(VI) solution was adsorbed on 0.2 g nanocomposites for 30 min and then desorbed with 20 mL of 0.01 M NaOH solution for 1 h. After each cycle of adsorption-desorption, the nanocomposites were washed thoroughly with ultrapure water to neutrality and reconditioned for adsorption in the succeeding five cycles.

3. Results and Discussion

3.1. Characterization of Materials. Shown in Figure 1 are the TEM micrographs of the obtained Fe/Mn mixed metal

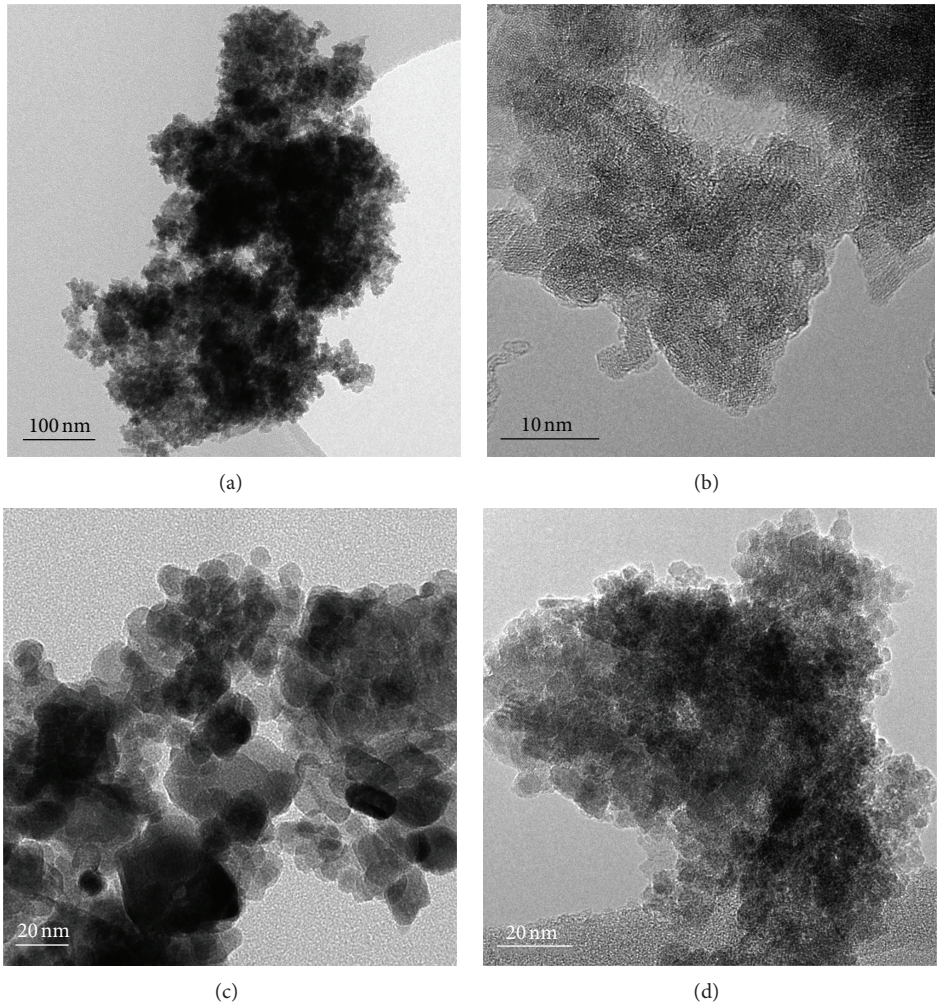

Figure 1: TEM pictures of Fe/Mn mixed metal oxide ((a), (b)), Mn_3O_4 (c), and Fe_2O_3 (d) nanoparticles.

oxide nanocomposites, Mn_3O_4 nanoparticles, and Fe_2O_3 nanoparticles. From Figure 1(a), it can be seen that the resultant composites were comprised of nanoparticles and these nanoparticles were aggregated together. Figure 1(b) is the HRTEM picture of the obtained nanocomposites. We can see that the diameter of these nanoparticles is about 3–5 nm and not well-crystallized. These nanoparticles were difficult to be distinguished. Figures 1(c) and 1(d) show the TEM pictures of the controlled experiments prepared by adding $Fe(NO_3)_3{\cdot}6H_2O$ or $MnCl_2{\cdot}4H_2O$ only. Figure 1(c) showed the obtained Mn_3O_4 nanoparticles. The picture presented that the Mn_3O_4 nanoparticles were highly crystalline and the diameter of the particles is about 10–50 nm, which is larger than that of mixed Fe/Mn metal oxides. Meanwhile, when using $Fe(NO_3)_3{\cdot}6H_2O$ as the only starting material, the Fe_2O_3 nanoparticles with a diameter of about 3–7 nm were obtained and these nanoparticles were also aggregated, as shown in Figure 1(d). By comparison of these four pictures, it was shown that the morphology of the mixed metal oxides was similar to that of Fe_2O_3 nanoparticles. Furthermore, we did not see any particles with size of more than 10 nm. This observation implied that the size of Mn_3O_4 nanoparticles was reduced and the crystallinity was affected when using both $Fe(NO_3)_3{\cdot}6H_2O$ and $MnCl_2{\cdot}4H_2O$ as the starting material.

XRD characterization was performed to determine the crystalline structure of these composites and the results were shown in Figure 2. For the sample prepared using $MnCl_2{\cdot}4H_2O$ as the starting material, the diffraction pattern in Figure 2(a) agreed well with those for standard Mn_3O_4 (JCPDS 18-0803). For the sample prepared using $Fe(NO_3)_3{\cdot}6H_2O$ as the starting material, the diffraction peaks of as-synthesized products match well with those of Fe_2O_3 (JCPDS 25-1402), although the nanoparticles are not well-crystallized. However, when using both $Fe(NO_3)_3{\cdot}6H_2O$ and $MnCl_2{\cdot}4H_2O$ as the starting material, only a weak diffraction peak was detected for the prepared composites, as shown in Figure 2(c). This observation indicated that Fe/Mn mixed metal oxide nanocomposite was not well-crystallized, which was consistent with the TEM observations. Moreover, we found that adding of $Fe(NO_3)_3{\cdot}6H_2O$ led to the amorphous structure of the composites. Thus, owing to the not well-crystallized structure and small size of the sample, it was

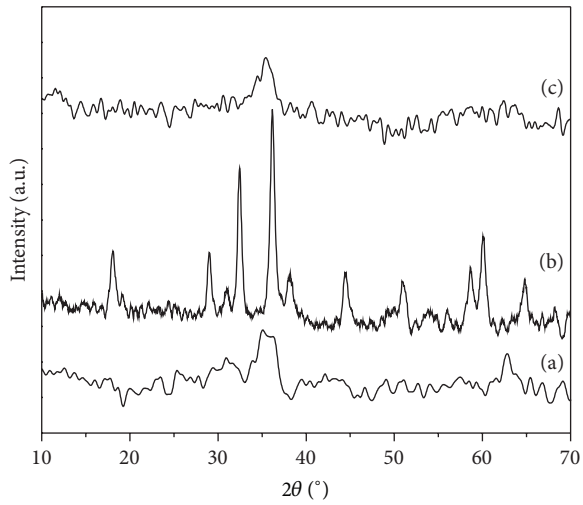

Figure 2: XRD patterns of Mn_3O_4 (a), Fe_2O_3 (b), and Fe/Mn mixed metal oxide (c) nanoparticles.

difficult to determine the exact structure of the obtained composite. In such a process, there were two possible products. One is to form $MnFe_2O_4$ nanoparticles. The other is mixed metal oxide composites. Due to the thermodynamic behavior of the $MnFe_2O_4$ nanoparticles [21] and the synthetic condition in our experiment, the obtained composites can only be made of mixed metal oxides. From the TEM and XRD analysis above, we speculated that the resultant composites may be made up of not well-crystallized Fe_2O_3 and Mn_3O_4 nanoparticles. However, this speculation has to be evidenced.

XPS characterization was involved to determine the structure. Figure 3 shows the XPS overall spectrum and the Mn_{2p} and Fe_{2p} spectra of the synthesized composites. The surface analysis indicated that only Fe, Mn, O, and C existed on the sample surface, implying that no other impurities existed in the product. The peak at 285.0 eV comes from the deposited carbon. From the Fe_{2p} spectra, the XPS peaks have a binding energy of 711.3 eV and a satellite feature centered at 719.9 eV, which is indicative of Fe(III) [3]. It can be concluded that only fully oxidized iron was on the sample. For the Mn species, the Mn $2p_{3/2}$ binding energy is 641.9 eV and Mn $2p_{1/2}$ binding energy is 653.6 eV, coming from Mn $2p_{3/2}$ and Mn $2p_{1/2}$ of Mn_3O_4, which was in accordance with [21]. This result indicates that the $MnCl_2{\cdot}4H_2O$ species were fully oxidized into Mn_3O_4. Based on the aforementioned characterizations, it could be suggested that the synthesized composites were mixed metal oxides composed of Fe_2O_3 and Mn_3O_4. These results also demonstrated the efficiency of the grinding method for preparation of the mixed metal oxide composites.

3.2. Adsorption Kinetic Study. The as-synthesized composites were used as adsorbents for Cr(VI) removal. Figure 4 showed the effect of contact time on the adsorption of Cr(VI). It can be seen that the uptake of Cr(VI) was finished within 10 min with 93% of the Cr(VI) removed during the first minute of the reaction. The equilibrium time is independent of the initial concentration of Cr(VI). The rapid adsorption of Cr(VI) by the composite is different from the microporous adsorption process. It is perhaps caused by external surface adsorption which is easy to access, while adsorption sites occurred in the exterior of porous adsorbents during the microporous adsorption process. At equilibrium, the adsorption capacities of Cr(VI) at initial concentrations of 50 and 150 mg/L were found to be 9.62 and 26.30 mg/g, respectively.

Compared with another oxide and their composites reported, the Fe/Mn mixed oxides nanocomposites were found to show higher adsorption capacity, as shown in Table 1. At the same time, the adsorption capacity and BET surface areas of the Fe/Mn mixed oxides nanocomposites were strongly dependent on the ratio of $MnCl_2{\cdot}4H_2O$ to KCl. For a grinding process, it is generally accepted that the necessary condition taking place in solid state reaction at room temperature is that one of the reactants should have crystalline waters or a low melting point on one hand, whilst on the other hand sufficient grinding is also required to provide the reactant molecules with more contact opportunities [22]. When the salts with crystalline water and other reactants were reacted, a layer of liquid film over particles was considered to be formed to construct a micro-aqueous-environment. Hereby, KCl and free water are expected to give a saturated solution of KCl. Then KCl was released to produce a shell surrounding the nanoparticles to prevent them from aggregating into larger particles [23]. Thus, the higher the $MnCl_2{\cdot}4H_2O$ to KCl ratio, the lower the crystal size and the higher BET surface areas. Secondly, the adsorption capacity of Fe/Mn mixed oxides composites was higher compared with separated γ-Fe_2O_3 and Mn_3O_4. At the same time, we mixed the γ-Fe_2O_3 and Mn_3O_4 metal oxides together with Fe : Mn mole ratio equal to 2. The mixed adsorption capacity for Cr(VI) removal is lower than the prepared Fe/Mn mixed metal oxides. We speculated that the enhanced adsorption capacity may be caused by the synergistic effect of the mixed metal oxides.

3.3. Adsorption Isotherm. The adsorption isotherm experimental results for Cr(VI) on composites at pH 2, 7, and 10 and different initial Cr(VI) concentrations were shown in Figure 5. It was revealed that Cr(VI) uptake increased with the initial Cr(VI) concentrations for the composite. The equilibrium adsorption capacity decreased with an increase in pH, which indicates that the lower pH favors adsorption. The results were accordant with the results reported by Chen and his group [16, 17]. It appears that adsorption isotherms on the composites can be well described by the Langmuir equation.

3.4. Adsorbent Stability. To test the stability of the resultant composites, desorption and regeneration experiments were carried out. Figure 6 shows the reusability of the composites for Cr(VI) removal. For the desorption process, 0.01 M NaOH eluant was used and more than 95% of Cr(VI) could be removed from the adsorbent of nanocomposites within 1 h. The adsorbent was recovered by filtration and drying. Recovered nanocomposites were reused again for the adsorption

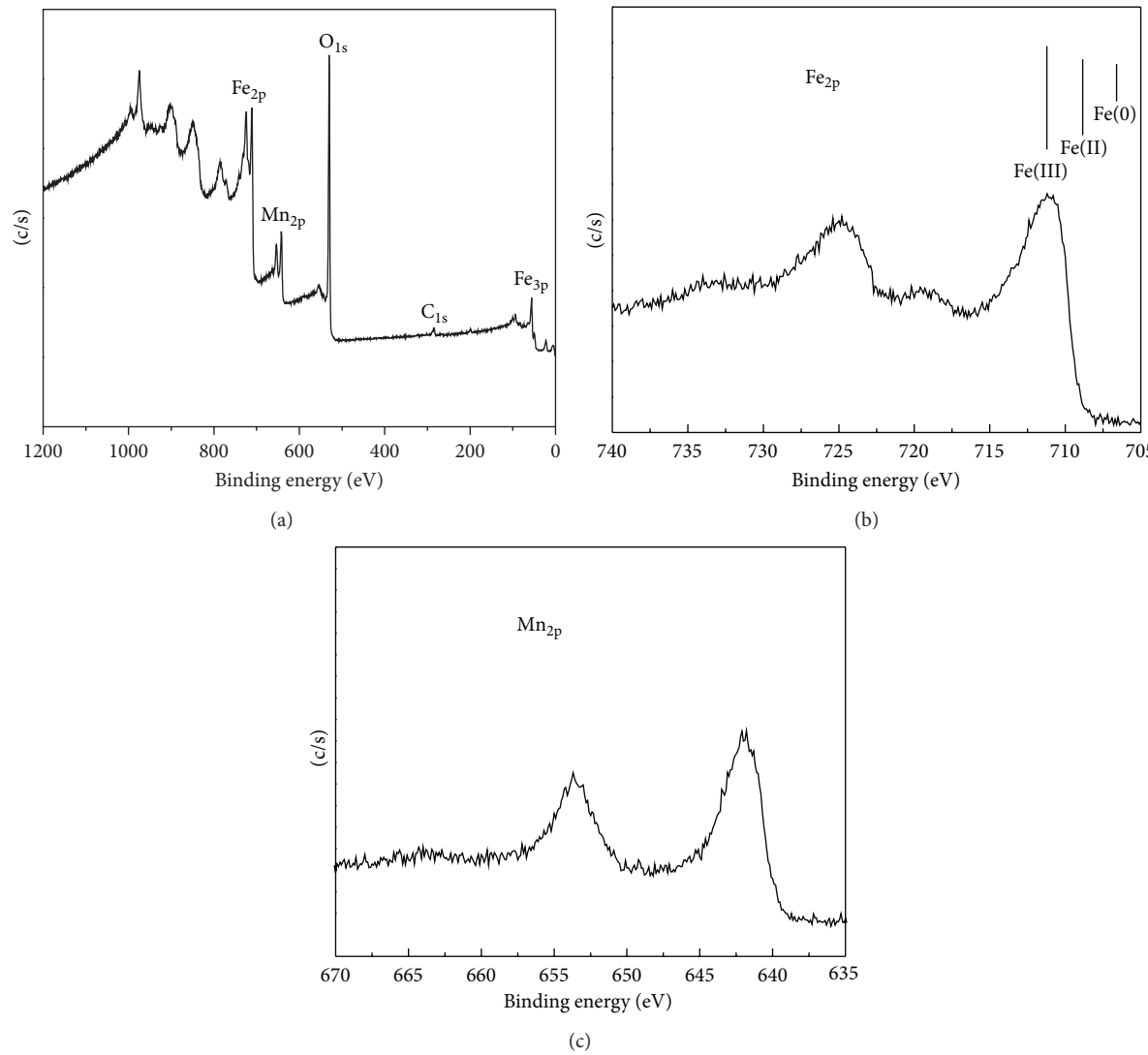

Figure 3: XPS spectra of Fe/Mn mixed metal oxides, (a) overall scan, (b) Fe_{2p} scan, and (c) Mn_{2p}.

of Cr(VI) and the adsorption capacity was tested. After 5 runs, the adsorption capacity tended to become steady. In the fifth cycle, the adsorption capacity was 25.3 mg/g which was 92% of the first cycle. The results indicated that the composites showed good stability and regeneration ability. In addition to chromium, iron and manganese were measured using ICP after each adsorption/desorption process, and the concentrations of these two metals were found to be nearly zero, indicating that the dissolution of the nanoparticles under the stated experimental conditions can be neglected.

3.5. Adsorbent Mechanism. For the removal of Cr(VI) from metal oxides, two commonly used mechanisms were reported by other researchers [16, 18]. One is the electrostatic attraction; the other is ion exchange. To find out any possible mechanism for Cr(VI) removal from the nanocomposites, the XPS characterization for the adsorption process was conducted. The first problem needed to be excluded is the valence change of the chromium during the adsorption process. If the valence of the chromium changed from hexavalent to trivalent, it means that a chemical redox reaction happened and the whole process was not an adsorption process. Figure 7 showed the XPS spectra of Cr, Fe, and Mn species before adsorption and after adsorption at pH equal to 2. The peak for Cr $2p_{3/2}$ was centered at 579.8 eV and the peak for Cr $2p_{1/2}$ was centered at 587.2 eV, and both were entirely from Cr(VI) [24]. The Fe $2p_{3/2}$ spectrum registered at 711.5 eV, and the Fe $2p_{1/2}$ spectrum registered at 724.3 eV in the XPS spectra, which indicated fully oxidized iron on the surface. Mn $2p_{3/2}$ and Mn $2p_{1/2}$ peaks centered at 641.9 eV and 653.6 eV, respectively, which came from Mn_3O_4. However, the valence of the adsorbed chromium was not changed and the valence of manganese should not vary, because iron is fully oxidative. Thus, it can be suggested that there is no chemical redox reaction occurring in the adsorption process. But this does not mean that the electrostatic attraction is the only mechanism in the adsorption process. When pH is greater than pH_{zpc} (=6.5), no Cr(VI) should be adsorbed on

Table 1: BET surface areas and removal capacity of different kinds of adsorbent samples.

Adsorbent samples	BET surface area ($m^2 \cdot g^{-1}$)	Adsorption capacity for Cr(VI) ($mg \cdot g^{-1}$)
Fe_2O_3-Mn_3O_4 (1 : 0)*	187	22.9
Fe_2O_3-Mn_3O_4 (1 : 2.5)*	213	21.3
Fe_2O_3-Mn_3O_4 (1 : 5)*	222	21.2
Fe_2O_3-Mn_3O_4 (1 : 10)*	264	24.6
Fe_2O_3-Mn_3O_4 (1 : 15)*	268	26.3
Mn_3O_4	61	11.6
γ-Fe_2O_3 [15]	178	19.4
Fe_3O_4	198	21.0
$MnFe_2O_4$(MnO_2 and Fe_2O_3) [14]	208	31.3

*Different ratio of $MnCl_2$ to KCl in the preparation.

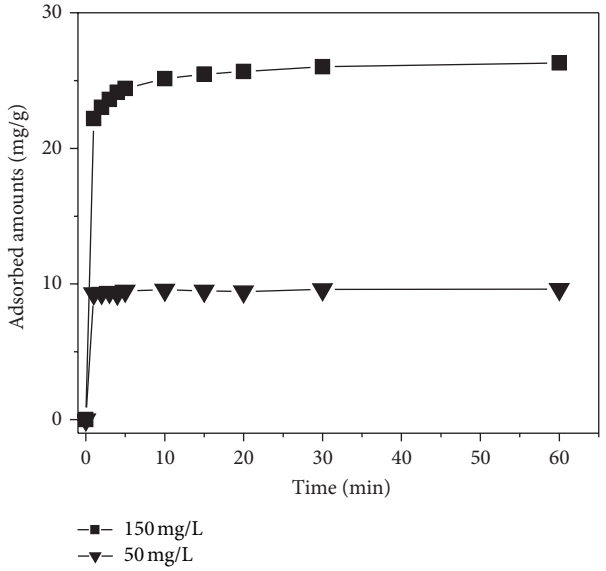

Figure 4: Kinetic study of Cr(VI) adsorption onto the Fe/Mn mixed metal oxides.

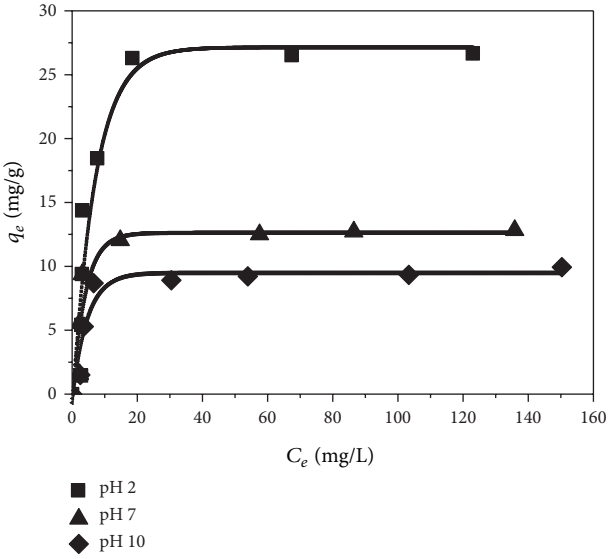

Figure 5: Langmuir isotherms of Cr(VI) adsorption onto the Fe/Mn mixed metal oxides at different pH.

the composites owing to the electrostatic repulsion. However, a certain amount of Cr(VI) ions was still adsorbed on the composites when the pH equal to 10. Therefore, there should be another mechanism involved in the chemical process. At pH greater than pH_{zpc} (=6.5), it is reported that the chromate can replace hydroxide from the surface of the hydrolyzed metal oxides as a result of the higher affinity of chromate ions with metal oxides than that of hydroxides with metal oxide [25]. Thus, it is concluded that the adsorption mechanism on the composite is the combination of electrostatic attraction and ion exchange.

4. Conclusion

In conclusion, Fe/Mn mixed metal oxide nanocomposites were successfully prepared using a grinding method at room temperature. The characterization results revealed that

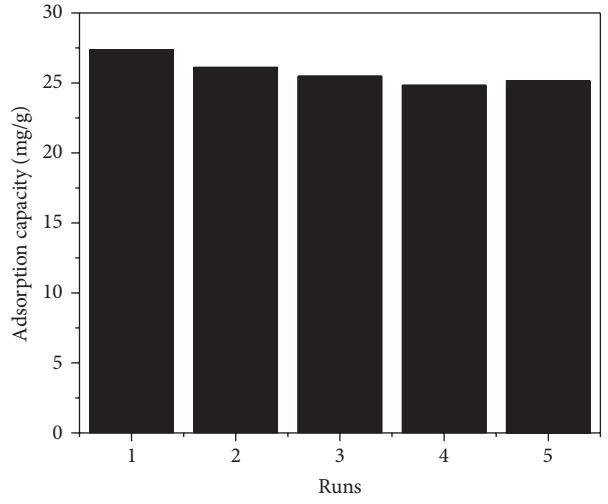

Figure 6: Regeneration studies of Fe/Mn mixed metal oxides after five cycles.

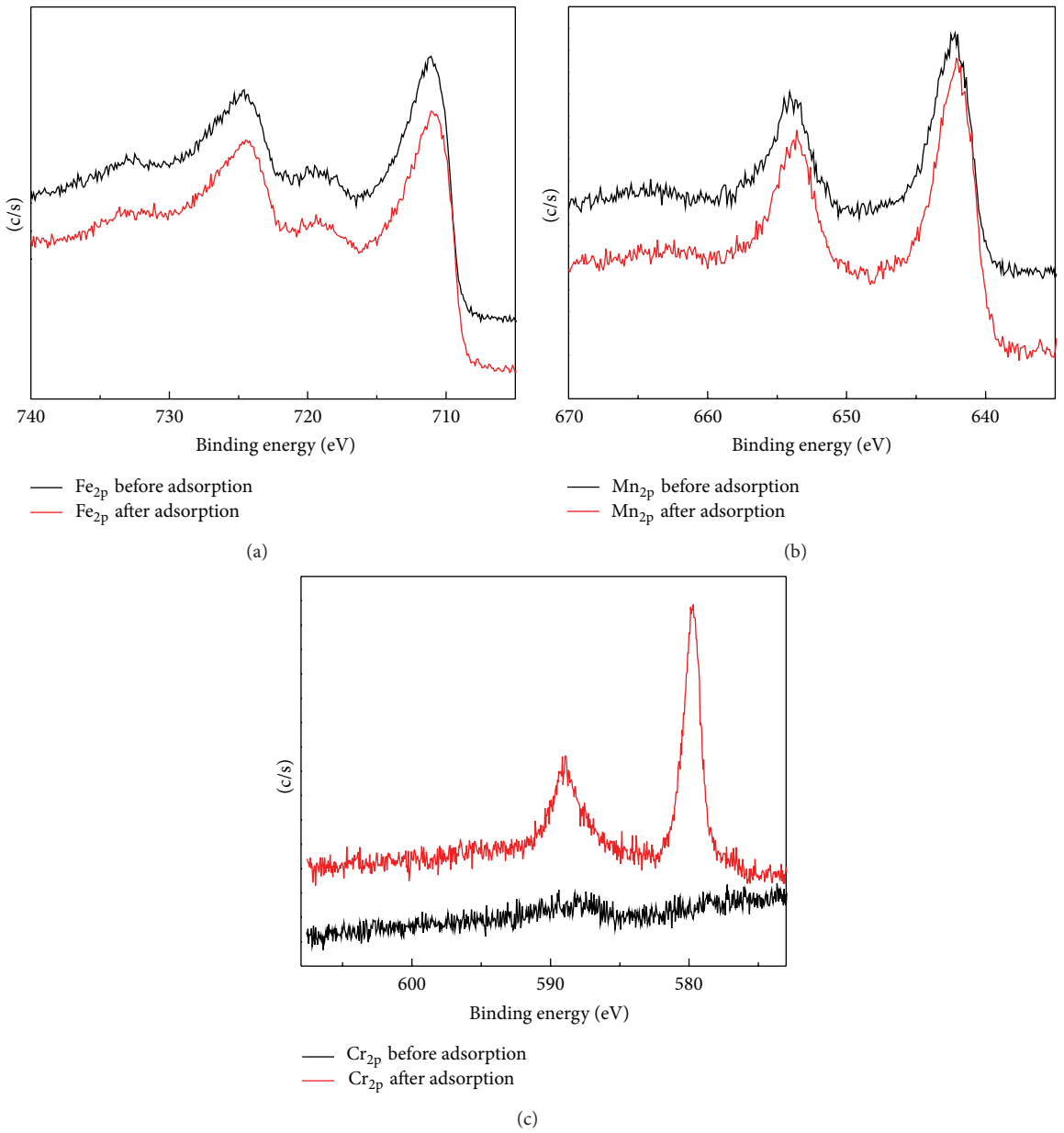

FIGURE 7: XPS spectra of Fe/Mn mixed metal oxides (a) before and (b) after adsorption of Cr(VI).

the as-synthesized composites were comprised of not well-crystallized Fe_2O_3 and Mn_3O_4 nanoparticles with a diameter about 3–5 nm. Compared with other oxides and their composites, the obtained composite was a very attractive adsorbent for the removal of the Cr(VI). The enhancement of the adsorption capacity was attributed to its higher BET surfaces and the synergistic effect coming from the mixed metal oxides. The resultant composite also showed good stability and regeneration activity. Combining the XPS results in the adsorption process, the mechanism for Cr(VI) removals on the composites was found to be a combination of electrostatic attraction and ion exchange. The new Fe/Mn mixed metal oxide composites synthesized in this work demonstrated a great potential application in the Cr(VI) removal.

Acknowledgments

The authors would like to acknowledge the funding support of Natural Science Foundation of Guangdong Province (S2012040007694), China Postdoctoral Science Foundation (20110490942), Fundamental Research Funds for the Central Universities (no. 11612328) and National Natural Science Foundation of China (51106185).

References

[1] M. J. Zamzow, B. R. Eichbaum, K. R. Sandgren, and D. E. Shanks, "Removal of heavy metals and other cations from wastewater using zeolites," *Separation Science and Technology*, vol. 25, no. 13–15, pp. 1555–1569, 1990.

[2] R. J. Crawford, I. H. Harding, and D. E. Mainwaring, "Adsorption and coprecipitation of multiple heavy metal ions onto the hydrated oxides of iron and chromium," *Langmuir*, vol. 9, no. 11, pp. 3057–3062, 1993.

[3] S. R. Qiu, H. F. Lai, M. J. Roberson et al., "Removal of contaminants from aqueous solution by reaction with iron surfaces," *Langmuir*, vol. 16, no. 5, pp. 2230–2236, 2000.

[4] R. Apak, E. Tütem, M. Hügül, and J. Hizal, "Heavy metal cation retention by unconventional sorbents (red muds and fly ashes)," *Water Research*, vol. 32, no. 2, pp. 430–440, 1998.

[5] N. Ballav, A. Maity, and S. B. Mishra, "High efficient removal of chromium(VI) using glycine doped polypyrrole adsorbent from aqueous solution," *Chemical Engineering Journal*, vol. 198, pp. 536–546, 2012.

[6] S. R. Singh and A. P. Singh, "Treatment of water containg chromium (VI) using rice husk carbon as a newlow cost adsorbent," *International Journal of Environmental Research*, vol. 6, pp. 917–924, 2012.

[7] J. Wang, L. Zhao, W. J. Duan, L. L. Han, and Y. F. Chen, "Adsorption of aqueous Cr(VI) by novel fibrous adsorbent with amino and quaternary ammonium groups," *Industrial & Engineering Chemistry Research*, vol. 51, pp. 13655–13662, 2012.

[8] S. J. Ergas, B. M. Therriault, and D. A. Reckhow, "Evaluation of water reuse technologies for the textile industry," *Journal of Environmental Engineering*, vol. 132, no. 3, pp. 315–323, 2006.

[9] S. R. Chowdhury, E. K. Yanful, and A. R. Pratt, "Chemical states in XPS and Raman analysis during removal of Cr(VI) from contaminated water by mixed maghemite-magnetite nanoparticles," *Journal of Hazardous Materials*, vol. 235, pp. 246–256, 2012.

[10] D. C. Sharma and C. F. Forster, "Removal of hexavalent chromium from aqueous solutions by granular activated carbon," *Water SA*, vol. 22, no. 1, pp. 153–160, 1996.

[11] Y. S. Ho, D. A. J. Wase, and C. F. Forster, "Kinetic studies of competitive heavy metal adsorption by sphagnum moss peat," *Environmental Technology*, vol. 17, no. 1, pp. 71–77, 1996.

[12] H. C. P. Srivastava, R. P. Mathur, and I. Mehrotra, "Removal of chromium from industrial effluent by adsorption on sawdust," *Environmental Technology Letters*, vol. 7, no. 1, pp. 55–63, 1986.

[13] L. S. Zhong, J. S. Hu, H. P. Liang, A. M. Cao, W. G. Song, and L. J. Wan, "Self-assembled 3D flowerlike iron oxide nanostructures and their application in water treatment," *Advanced Materials*, vol. 18, no. 18, pp. 2426–2848, 2006.

[14] L. S. Zhong, J. S. Hu, A. M. Cao, Q. Liu, W. G. Song, and L. J. Wan, "3D flowerlike ceria micro/nanocomposite structure and its application for water treatment and CO removal," *Chemistry of Materials*, vol. 19, no. 7, pp. 1648–1655, 2007.

[15] J. Hu, G. Chen, and I. M. C. Lo, "Selective removal of heavy metals from industrial wastewater using maghemite nanoparticle: performance and mechanisms," *Journal of Environmental Engineering*, vol. 132, no. 7, pp. 709–715, 2006.

[16] J. Hu, G. Chen, and I. M. C. Lo, "Removal and recovery of Cr(VI) from wastewater by maghemite nanoparticles," *Water Research*, vol. 39, no. 18, pp. 4528–4536, 2005.

[17] J. Hu, I. M. C. Lo, and G. Chen, "Fast removal and recovery of Cr(VI) using surface-modified jacobsite ($MnFe_2O_4$) nanoparticles," *Langmuir*, vol. 21, no. 24, pp. 11173–11179, 2005.

[18] J. Hu, I. M. C. Lo, and G. Chen, "Performance and mechanism of chromate (VI) adsorption by δ-FeOOH-coated maghemite (γ-Fe_2O_3) nanoparticles," *Separation and Purification Technology*, vol. 58, no. 1, pp. 76–82, 2007.

[19] V. V. Molchanov and R. A. Buyanov, "Mechanochemistry of catalysts," *Russian Chemical Reviews*, vol. 69, no. 5, pp. 435–450, 2000.

[20] K. Muthukumaran, N. Balasubramanian, and T. V. Ramakrishna, "Removal and recovery of chromium from plating waste using chemically activated carbon," *Metal Finishing*, vol. 93, no. 11, pp. 46–53, 1995.

[21] G. Bonsdorf, K. Schäfer, K. Teske, H. Langbein, and H. Ullmann, "Stability region and oxygen stoichiometry of manganese ferrite," *Solid State Ionics*, vol. 110, no. 1-2, pp. 73–82, 1998.

[22] Q. Li, G. Luo, J. Li, and X. Xia, "Preparation of ultrafine MnO_2 powders by the solid state method reaction of $KMnO_4$ with Mn(II) salts at room temperature," *Journal of Materials Processing Technology*, vol. 137, no. 1–3, pp. 25–29, 2003.

[23] J. Lu, S. Yang, K. M. Ng et al., "Solid-state synthesis of monocrystalline iron oxide nanoparticle based ferrofluid suitable for magnetic resonance imaging contrast application," *Nanotechnology*, vol. 17, no. 23, pp. 5812–5820, 2006.

[24] M. Ding, B. H. W. S. De Jong, S. J. Roosendaal, and A. Vredenberg, "XPS studies on the electronic structure of bonding between solid and solutes: adsorption of arsenate, chromate, phosphate, Pb^{2+}, and Zn^{2+} ions on amorphous black ferric oxyhydroxide," *Geochimica et Cosmochimica Acta*, vol. 64, no. 7, pp. 1209–1219, 2000.

[25] M. Dimitri, G. Vladimir, and W. Abraham, *Ion Exchange*, Marcel Dekker, New York, NY, USA, 2000.